Miner Deposita (2010) 45:3–9
DOI 10.1007/s00126-009-0259-x

LETTER

Precise U–Pb zircon–baddeleyite age of the Jinchuan sulfide ore-bearing ultramafic intrusion, western China

Mingjie Zhang · Sandra L. Kamo · Chusi Li · Peiqing Hu · Edward M. Ripley

Received: 24 April 2009 / Accepted: 16 August 2009 / Published online: 1 September 2009

Abstract The Jinchuan ultramafic intrusion in western China hosts the third-largest magmatic Ni–Cu deposit in the world. The crystallization age of the intrusion has long been debated. Here, we present a U–Pb ID-TIMS zircon age of 831.8±0.6 Ma obtained on thermally annealed and chemically etched zircons from a lherzolite sample. The coexisting baddeleyite in the sample is indistinguishable from the age of zircon. Our new results confirm that the emplacement of the Jinchuan ultramafic intrusion was temporally related to the breakup of the Rodinia supercontinent.

Keywords Zircon · Baddeleyite · U–Pb dating · ID-TIMS · Jinchuan · China · Ni deposit

Introduction

The Jinchuan Ni–Cu deposit in western China is the third-largest magmatic sulfide deposit in the world (Naldrett 2009). It contains >500 million metric tons of sulfide ores with grades of 1.1 wt.% Ni and 0.7 wt.% Cu (Chai and Naldrett 1992a; Tang et al. 2009). The ages of the Jinchuan ultramafic intrusion and associated sulfide mineralization have been debated for a long time. Tang et al. (1992) and Zhang et al. (2004) reported Sm–Nd isochron ages of 1,508±31 and 970±310 Ma, respectively, for the Jinchuan ultramafic intrusion. Yang et al. (2005, 2008) and Yan et al. (2005) reported Re–Os isochron ages of 1,220±57 to 833±35 Ma for the sulfide ores of the intrusion. Li et al. (2004b, 2005) reported a U–Pb SHRIMP zircon age of 827±8 Ma and a U–Pb SHRIMP baddeleyite age of 812±26 Ma for the Jinchuan ultramafic intrusion. Li et al. (2005) also reported a U–Pb SHRIMP zircon age of 828±3 Ma for a diorite dike that cuts the Jinchuan ultramafic intrusion. Using the same method, Yan et al. (2005) obtained an age of ~837 Ma for zircon from the Jinchuan ultramafic intrusion, but they interpreted it as a metamorphic age instead of a primary magmatic age. More recently, Tian et al. (2007) reported a LA-ICP-MS zircon U–Pb age of 807.3±3.7 Ma for the Jinchuan ultramafic intrusion. In this communication, we present a more precise U–Pb ID-TIMS zircon age for the Jinchuan ultramafic intrusion using the chemical abrasion pre-treatment (Mattinson 2005). We also present U–Pb baddeleyite data from the same sample. We hope that our new data will resolve the dispute about the age of the Jinchuan ultramafic intrusion.

Geological background

The Jinchuan ultramafic intrusion is one of several mafic–ultramafic intrusions within the Longshoushan uplifted terrane situated along the southwestern margin of the North China Craton (Fig. 1). The Longshoushan terrane consists of Paleoproterozoic amphibolites, migmatites, and gneisses, overlain by Late Mesoproterozoic sedimentary rocks that

Editorial handling: R. Romer.

M. Zhang · P. Hu
MOE Key Laboratory of Western China's Environmental Systems, Lanzhou University,
Lanzhou 730000, China

S. L. Kamo
Jack Satterly Geochronology Laboratory, Department of Geology,
University of Toronto,
Toronto, Canada M5S 3B1

C. Li (✉) · E. M. Ripley
Department of Geological Sciences, Indiana University,
Bloomington, IN 47405, USA
e-mail: cli@indiana.edu

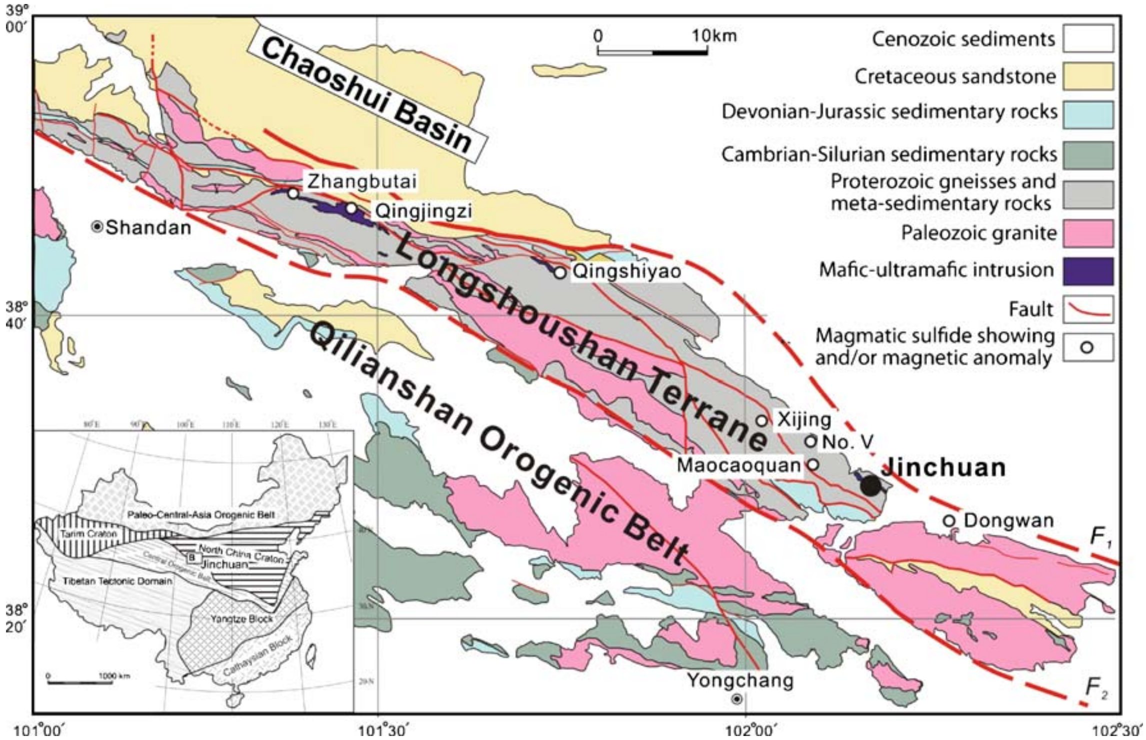

Fig. 1 Simplified maps showing the tectonic units of China (*inset*) and regional geology of Jinchuan area. Modified from Tang et al. (2009)

have experienced greeschist-grade metamorphism (SGU 1984). The Longshoushan terrane is bounded by the North Qilianshan tectonic suture zone of ~450 Ma (Song et al. 2006a) to the south. Large Paleozoic granite plutons occur across the boundary between the North Qilianshan suture zone and the Longshoushan terrane.

The Jinchuan ultramafic intrusion is a dike-like body (~6,500 m long, <500 m wide, and >1,100 m deep in its central part) dominated by olivine-rich rocks such as harzburgite, lherzolite, and dunite. Immediate country rocks of the Jinchuan ultramafic intrusion are Lower Proterozoic migmatites, gneisses, and marbles (SGU 1984; Fig. 2a). It is divided into several segments by a series of northeast-trending strike–slip faults. Sulfide mineralization occurs in the lower parts of the intrusion mainly in the form of disseminated and net-textured ore with pyrrhotite, chalcopyrite, and pentlandite (Fig. 2b).

Previous studies of the Jinchuan sulfide ore-bearing ultramafic intrusion have led to conflicting theories with respect to magma evolution and sulfide genesis. Chai and Naldrett (1992b) proposed that the Jinchuan intrusion was the root zone of a much larger layered intrusion and that the dike-like central part of the intrusion was a feeder to the magma chamber. Tang (1993) suggested that the Jinchuan intrusion formed by multiple inputs from a deep-seated stratified magma chamber. Sulfide-bearing magma was proposed to have been extracted from the lower portion of the deep chamber, whereas sulfide-barren intrusions were extracted from the upper portion. Li et al. (2004a) and de Waal et al. (2004) showed, using trace elements and olivine composition, that emplacement involved high-viscosity, dense, crystal-rich mushes. Several pulses of magma are required to explain the variations in olivine composition, and flow and gravitational differentiation of a sulfide-rich magma are thought to account for the present distribution of textural features. Like Tang (1993), de Waal et al. (2004) and Song et al. (2009) call upon emplacement of sulfide-bearing and sulfide-free pulses from a deep, stratified magma chamber to explain the occurrence of sulfide-barren as well as sulfide-bearing rocks in the Jinchuan area. Lehmann et al. (2007) proposed that the Jinchuan ultramafic intrusion was emplaced as a sill along an unconformity between high-grade gneisses and marbles.

Chai and Naldrett (1992b) and Lehmann et al. (2007) suggested that the parental magma of the Jinchuan intrusion was high-Mg basalt instead of ultramafic magma, which many Chinese geologists initially accepted. Li et al. (2005) suggested that the parental magma of the Jinchuan intrusion was derived from the subcontinental lithospheric mantle and experienced crustal contamination based on negative $\varepsilon_{\mathrm{Nd}}$ values (−9 to −12) that decrease with increasing La/Sm. Song et al. (2006b) and Lehmann et al. (2007) reported negative Nb and Ta anomalies in the Jinchuan rocks and attributed these anomalies to crustal contamination. Song et al. (2006b, 2009) proposed that sulfide saturation was achieved at depth as a result of

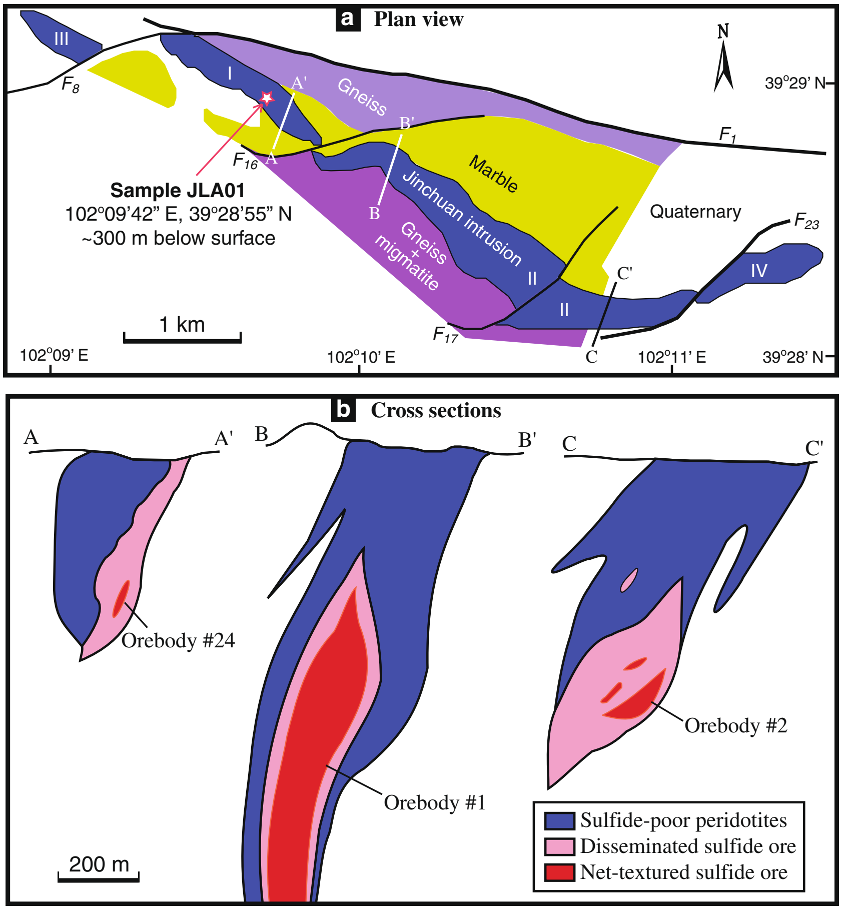

Fig. 2 Plan view (**a**) and cross sections (**b**) of the Jinchuan sulfide ore-bearing ultramafic intrusion. Modified from SGU (1984)

fractional crystallization as well as crustal contamination. Lehmann et al. (2007) suggested that sulfide saturation was induced by the addition of carbonate-rich fluids, which increased the oxygen fugacity of the magma and thereby decreased the maximum solubility of sulfur in the magma.

Post-magmatic hydrothermal alteration and metamorphism of the Jinchuan intrusion and sulfide ores have been recognized by many researchers (Chai and Naldrett 1992a; Barnes and Tang 1999; Li et al. 2004a; Ripley et al. 2005; Yang et al. 2006), and have made it difficult to accurately interpret the whole rock PGE compositions (Yang et al. 2006; Su et al. 2008; Song et al. 2009), S–O–H isotopes (Ripley et al. 2005), Nd–Sr isotopes (Tang et al. 1992; Zhang et al. 2004) and Re–Os isotopes (Yang et al. 2008).

Sampling and analytical methods

A sample of sulfide-poor lherzolite (~15 kg) was collected underground in the western part of the Jinchuan ultramafic intrusion (Fig. 2a). This is one of the least-altered samples from the intrusion we have seen. Minor serpentine alteration is present as small veins within olivine crystals and sporadic chlorite alteration is restricted to the margins of pyroxene crystals.

Zircon and baddeleyite grains were selected under a binocular microscope and examined for visible imperfections. Zircon grains were thermally annealed and chemically leached ("chemically abraded") prior to analysis by being placed in a muffle furnace for ~60 h to anneal damaged lattice sites, followed by leaching (partial dissolution) in hydrofluoric acid in Teflon dissolution vessels at 200°C for 6 h (Mattinson 2005). Grain weights were estimated using photomicrographs; uncertainties in weights affect only U and Pb concentrations and not age information. Grains were cleaned in room temperature 7 N HNO_3 and ultraclean acetone prior to dissolution, and either a ^{205}Pb–^{235}U spike or ^{205}Pb–^{233}U–^{235}U spike ("ET535" from the EARTHTIME project, see www.earth-time.org, which was used to facilitate inter-laboratory and inter-method age comparisons) was added to the Teflon dissolution capsules during sample loading. Zircon and baddeleyite were dissolved using ~0.10 ml of concentrated hydrofluoric acid (HF) and ~0.02 ml of 7 N HNO_3 in Teflon dissolution

Table 1 U–Pb data for chemically abraded zircon grains and a baddeleyite fragment from the Jinchuan ultramafic intrusion, western China

No.	Weight (mg)	U (ppm)	Th/U	Pb^{Tot} (pg)	Pb^{Com} (pg)	$^{207}Pb/^{204}Pb$ measured	$^{207}Pb/^{235}U$	2 δ	$^{206}Pb/^{238}U$	2 δ	Error Corr	$^{206}Pb/^{238}U$ Age (Ma)	2 δ	$^{207}Pb/^{235}U$ Age (Ma)	2 δ	$^{207}Pb/^{206}Pb$ Age (Ma)	2 δ	% Disc
Zircon																		
1[a]	8.5	327	1.4	503.2	1.8	930	1.2740	0.0035	0.13797	0.00031	0.903	833.2	1.8	834.2	1.5	836.8	2.5	0.47
2[a]	3.8	197	2.2	154.5	0.5	861	1.2716	0.0028	0.13783	0.00022	0.855	832.4	1.3	833.1	1.3	835.1	2.5	0.35
3	3.0	121	2.4	77.5	0.5	431	1.2713	0.0027	0.13772	0.00024	0.836	831.7	1.4	833.0	1.2	836.2	2.5	0.57
4	11.0	251	2.5	595.5	0.8	2107	1.2699	0.0024	0.13770	0.00022	0.913	831.6	1.3	832.4	1.1	834.3	1.6	0.34
5	7.3	55	1.9	77.7	0.8	297	1.2713	0.0043	0.13762	0.00028	0.751	831.2	1.6	833.0	1.9	837.7	4.7	0.82
6	11.1	399	2.2	906.1	0.5	5301	1.2693	0.0030	0.13756	0.00027	0.935	830.8	1.5	832.1	1.3	835.4	1.8	0.58
7[a]	3.4	87	2.4	63.5	1.0	195	1.2588	0.0060	0.13676	0.00038	0.684	826.3	2.1	827.4	2.7	830.3	7.3	0.52
Baddeleyite																		
8	1.5	570	0.01	107.6	4.2	136	1.2627	0.0041	0.13697	0.00023	0.663	827.5	1.3	829.1	1.8	833.4	5.2	0.8

206/204 corrected for fractionation and common Pb in the spike. Correction for ^{230}Th disequilibrium in 206/238 and 207/206 assuming Th/U of 4.2 in the magma. Error correlation is correlation coefficients of *X–Y* errors on the concordia plot

Pb^{Tot} is the total amount of Pb excluding blank, Pb^{Com} is common Pb assuming the isotopic composition of laboratory blank: 206/204—18.221; 207/204—15.612; 208/204—39.360 (2σ errors of 2%), *Pb/U* ratios corrected for fractionation, common Pb in the spike, and blank, *Th/U* calculated from radiogenic $^{208}Pb/^{206}Pb$ ratio and $^{207}Pb/^{206}Pb$ age assuming concordance, *% Disc* is percent discordance for the given $^{207}Pb/^{206}Pb$ age

[a] Denotes analyses with ET535 spike solution, all others with University of Toronto spike solution

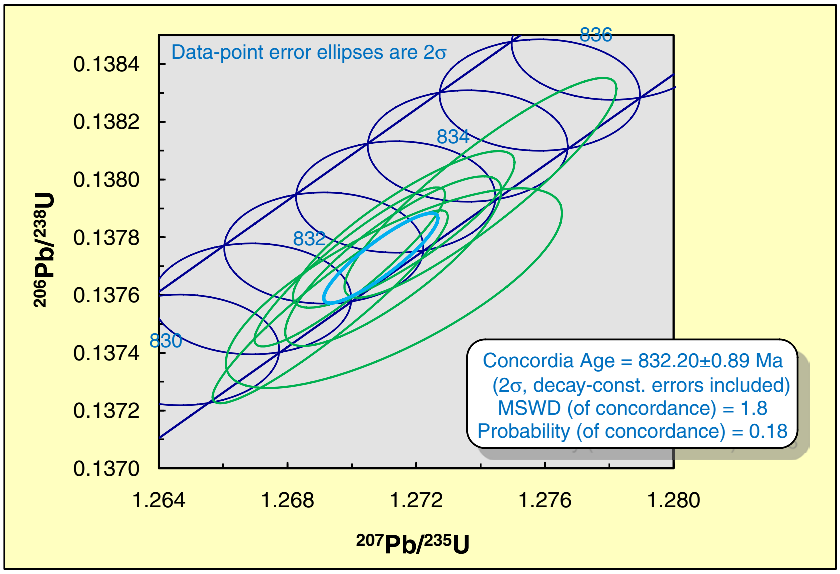

Fig. 3 Concordia plot of U–Pb data for chemically abraded single zircon grains from the Jinchuan ultramafic intrusion

bombs at 200°C (Krogh 1973) for 5 days, and then dried to a precipitate, followed by addition of ~0.08 ml of 3.1 N HCl overnight. U and Pb were isolated by using anion exchange column separation and loaded together onto outgassed rhenium filaments with silica gel (Gerstenberger and Haase 1997).

Pb and U were analyzed with a VG354 mass spectrometer using a Daly collector in pulse counting mode. All common Pb in zircon and baddeleyite was assigned to the isotopic composition of the laboratory Pb blank (see Table 1 footnotes). Dead time of the measuring system for Pb is 22.8 ns and 20.8 ns for U. The mass discrimination correction for the Daly detector is constant at 0.05%/amu. Amplifier gains and Daly characteristics were monitored using the SRM 982 Pb standard. Thermal mass discrimination corrections are 0.10%/amu.

Decay constants are those of Jaffey et al. (1971). All age errors quoted in the text and Table 1, and error ellipses in the Concordia diagram (Fig. 3) are given at the 95% confidence interval. Plotting and Concordia age calculation are from Isoplot 3.00 (Ludwig 2003).

Results

Six of seven U–Pb data for individual fragments of translucent, irregular-shaped zircon, pretreated by thermal annealing and chemical etching (chemical abrasion), are equivalent and plot immediately below the Concordia curve and within the U decay uncertainties (Fig. 3). These give a Concordia age (Ludwig 1998) of 832.20±0.89 Ma (2σ, decay constant errors included; MSWD of concordance and equivalence is 1.08; probability is 0.37), and a weighted mean ^{206}Pb/^{238}U of 831.8±0.6 Ma (2σ, decay constant errors included; MSWD=1.08; probability is 0.37; using Ludwig 2003). One analysis of chemically abraded zircon (analysis 7, see Table 1) plots just below the cluster, showing that despite the rigorous zircon pre-treatment, a small amount of Pb loss can persist and give too young a ^{206}Pb/^{238}U age, possibly due to an insufficient length of time for etching. A fragment of baddeleyite (analysis 8, see Table 1) overlaps the data for analysis 7, is 0.8% discordant, and has a ^{207}Pb/^{206}Pb age of 833.4±5.2 Ma, within error of the cluster of six data. Clustering of high-*n* data sets just below the Concordia curve has been observed previously in data from our laboratory (e.g., Black et al. 2003, 2004) and more extensively in Schoene et al. (2006). Interpreting the best age to report will continue to be a challenge as improvements to precision and accuracy, by eliminating trace amounts of Pb loss through grain pretreatment by chemical abrasion (Mattinson 2005), coupled with sub-picogram Pb procedural blanks, will result in data sets such as this being reported more commonly. The accuracy of the ages is dependent upon the accuracy of the two U decay constants. Begemann et al. (2001), Schön et al. (2004) and Schoene et al. (2006) have made the case for repeating the alpha-counting experiments of Jaffey et al. (1971); such an improvement is necessary in order to report the most accurate age for a mineral. For now, either the Concordia age, which considers the ^{207}Pb/^{206}Pb age and both Pb/U ages, or the weighted mean ^{206}Pb/^{238}U age of 831.8±0.6 Ma are the best age interpretations. Due to the lower abundance of ^{207}Pb, and its greater sensitivity to the laboratory blank isotopic composition, and less certainty in the accuracy of the ^{235}U decay constant (Mattinson 2000; Schoene et al. 2006), we favor the latter age interpretation.

Conclusions

We report a U–Pb ID-TIMS age of 831.8±0.6 Ma for a lherzolite sample from the Jinchuan ultramafic intrusion obtained from thermally annealed and HF-etched zircon crystals. A previously reported U–Pb zircon age that was determined using the LA-ICP-MS method (Tian et al. 2007) is ~25 My younger than our age and ~20 My younger than that obtained by the SHRIMP method (Li et al. 2004b, 2005). The new age is slightly older than that for a diorite dike that cuts the intrusion and was previously dated at 828±3 Ma by U–Pb SHRIMP (Li et al. 2005). Our new results support the conclusion of Li et al. (2005) that the emplacement of the Jinchuan ultramafic intrusion was temporally related to the breakup of the Rodinia supercontinent.

Acknowledgments This research was supported by the Natural Science Foundation of China (40534020) and Project-111 from the Ministry of Education of China (B07011).

References

Barnes SJ, Tang ZL (1999) Chrome spinel from the Jinchuan Ni-Cu sulfide deposit, Gansu province, People's Republic of China. Econ Geol 94:343–356

Begemann F, Ludwig KR, Lugmair GW, Min K, Nyquist LE, Patchett PJ, Renne P, Shih C-Y, Villa IM, Walker RJ (2001) Call for an improved set of decay constants for geochronological use. Geochim Cosmochim Acta 65:111–121

Black LP, Kamo SL, Allen CM, Aleinikoff JN, Davis DW, Korsch RJ, Williams IS, Foudoulis C (2003) TEMORA 1: a new zircon standard for Phanerozoic U–Pb geochronology. Chem Geol 200:155–170

Black LP, Kamo SL, Allen CM, Davis DW, Aleinikoff JN, Valley JW, Mundil R, Campbell IH, Korsch RJ, Williams IS, Foudoulis C (2004) Improved ^{206}Pb/^{238}U microprobe geochronology by the monitoring of a trace-element-related matrix effect; SHRIMP, ID-TIMS, ELA-ICP-MS and oxygen isotope documentation for a series of zircon standards. Chem Geol 205:115–140

Chai G, Naldrett AJ (1992a) Characteristics of Ni–Cu–PGE mineralization and genesis of the Jinchuan deposit, northwest China. Econ Geol 87:1475–1495

Chai G, Naldrett AJ (1992b) The Jinchuan ultramafic intrusion: cumulate of a high-MgO basaltic magma. J Petrol 33:277–303

de Waal SA, Xu ZH, Li C, Mouri H (2004) Emplacement of visceous mushes in the Jinchuan ultramafic intrusion, western China. Can Mineral 42:371–392

Gerstenberger H, Haase G (1997) A highly effective emitter substance for mass spectrometric Pb isotope ratio determinations. Chem Geol 136:309–312

Jaffey AH, Flynn KF, Glendenin LE, Bentley WC, Essling AM (1971) Precision measurement of half-lives and specific activities of ^{235}U and ^{238}U. Phys Rev 4:1889–1906

Krogh TE (1973) A low contamination method for hydrothermal decomposition of zircon and extraction of U and Pb for isotopic age determinations. Geochim Cosmochim Acta 37:485–494

Lehmann J, Arndt N, Windley B, Zhou M-F, Wang CY, Harris C (2007) Field relationships and geochemical constraints on the emplacement of the Jinchuan intrusion and its Ni–Cu–PGE sulfide deposit, Gansu, China. Econ Geol 102:75–94

Li C, Xu ZH, de Waal SA, Ripley EM, Maier WD (2004a) Compositional variations of olivine from the Jinchuan Ni–Cu sulfide deposit, western China: implications for ore genesis. Miner Depos 39:159–172

Li XH, Su L, Song B, Liu DY (2004b) SHRIMP zircon U–Pb age of the Jinchuan ultramafic intrusion and its geological significance. China Science Bulletin 49:420–422 (in Chinese)

Li XH, Su L, Chung SL, Li ZX, Liu Y, Song B, Liu DY (2005) Formation of the Jinchuan ultramafic intrusion and the world's third largest Ni-Cu sulfide deposit: Associated with the ~825 Ma south China mantle plume? Geochemistry Geophysics Geosystems: doi: 10.1029/2005GC001006

Ludwig KR (1998) On the treatment of concordant uranium–lead ages. Geochim Cosmochim Acta 62:665–676

Ludwig KR (2003) User's manual for Isoplot 3.00: a geochronological toolkit for Microsoft Excel. Berkeley Geochronology Center Special Publication No. 4, 71 pp

Mattinson JM (2000) Revising the "gold standard"—the uranium decay constants of Jaffey et al., 1971. Eos Trans. AGU, Spring Meet. Suppl., Abstract V61A-02

Mattinson JM (2005) Zircon U–Pb chemical abrasion ("CA-TIMS") method: combined annealing and multi-step partial dissolution analysis for improved precision and accuracy of zircon ages. Chem Geol 220:47–66

Naldrett AJ (2009) Fundamentals of Magmatic Sulfide Deposits. In: Li C, Ripley EM (eds) New developments in magmatic Ni–Cu and PGE deposits. Geological Publishing House, Beijing, pp 1–26

Ripley EM, Sarkar A, Li C (2005) Mineralogic and stable isotope studies of hydrothermal alteration at the Jinchuan Ni–Cu deposit, China. Econ Geol 100:1349–1361

Schoene B, Crowley JL, Condon DJ, Schmitz MD, Bowring SA (2006) Reassessing the uranium decay constants for geochronology using ID-TIMS U–Pb data. Geochim Cosmochim Acta 70:426–445

Schön R, Winkler G, Kutschera W (2004) A critical review of experimental data for the half-lives of the uranium isotopes ^{238}U and ^{235}U. Appl Radiat Isotopes 60:263–273

SGU (the Sixth Geological Unit of the Geological Survey of Gansu Province) (1984) Geology of the Baijiaozuizi Cu–Ni sulfide deposit. Geological Publishing House, Beijing, p 325

Song SG, Zhang LF, Niu YL, Su L, Song B, Liu DY (2006a) Evolution from oceanic subduction to continental collision: a case study for the northern Tibetan Plateau based on geochemical and geochronological data. J Petrol 47:435–455

Song X-Y, Zhou MF, Wang Y, Qi L (2006b) Role of crustal contamination in the formation of the Jinchuan Ni–Cu–PGE sulfide deposit, NW China. Int Geol Rev 48:1113–1132

Song X-Y, Keays RR, Zhou M-F, Qi L, Ihlenfeld C, Xiao JF (2009) Siderophile and chalcophile elemental constraints on the origin of the Jinchuan Ni–Cu–(PGE) sulfide deposit, NW China. Geochim Cosmochim Acta 73:404–424

Su SG, Li C, Zhou M-F, Ripley EM, Qi L (2008) Controls on variations of platinum-group element concentrations in the sulfide ores of the Jinchuan Ni–Cu deposit, western China. Miner Depos 43:609–626

Tang ZL (1993) Genetic model of the Jinchuan nickel–copper deposit. Geological Association of Canada Special Paper 40:389–401

Tang ZL, Yang J, Xu S, Tao S, Li W (1992) Sm–Nd dating of the Jinchuan ultramafic rock body, Gansu, China. Chin Sci Bull 37:1988–1991 (in Chinese)

Tang ZL, Song X-Y, Su SG (2009) Ni-Cu Deposits Related to High-Mg Basaltic Magma, Jinchuan, Western China. In: Li C, Ripley

EM (eds) New developments in magmatic Ni-Cu and PGE deposits. Geological Publishing House, Beijing, pp 121–140

Tian Y-L, Wu S-J, Meng R, Wang Y-S, Lin C-L, Xiao L-Z (2007) LA-ICPMS zircon U–Pb age of the Jinchuan ultramafic intrusion. Acta Mineralogica Sinica 27:211–217 (in Chinese with English abstract)

Yan H, Su S, Jiao J, Tang H (2005) Age of the Jinchuan Cu–Ni–(PGE) magmatic sulfide deposit. Earth Science Frontiers 12:309–315 (in Chinese with English abstract)

Yang G, Du A, Lu J, Qu W, Chen J (2005) Re–Os dating of massive sulfide ores of the Jinchuan Ni–Cu deposit by ICP-MS. Sci China (D) 35:241–245 (in Chinese)

Yang XZ, Ishihara S, Zhao DH (2006) Genesis of the Jinchuan PGE deposit, China: evidence from fluid inclusions, mineralogy and geochemistry of precious elements. Mineral Petrol 86:109–128

Yang S, Qu W, Tian Y, Chen J, Yang G, Du A (2008) Origin of the inconsistent apparent Re–Os ages of the Jinchuan Ni–Cu sulfide ore deposit, China: post-segregation diffusion of Os. Chem Geol 247:401–418

Zhang Z, Du A, Tang S, Lu J, Wang J, Yang G (2004) Age of the Jinchuan copper-nickel deposit and isotopic geochemical feature of its source. Acta geol Sin 78:359–365 (in Chinese with English abstract)